# Features of optical diffusion diagnostics in structure characterization of the foamed polymers

**Ushakova O.V.[1], Zimnyakov D.A.[1,2]**

**[1]Yury Gagarin State Technical University of Saratov, 77 Polytechnicheskayast., Saratov, 410054, Russia**

**[2] Institute for Problems of Precision Mechanics and Control RAS, 24 Rabochaya st., Saratov, 410028, Russia**

Various approaches to optical diffusion characterization of growing polymer foams as a specific version of multiple scattering random media with a high level of disorder are considered. These approaches include the diffuse reflectance and transmittance measurements, low-coherence reference-free and reference-based reflectometry, and full-field multi-speckle correlometry. The relationship between the key parameter of the optical diffusion diagnostics such as the transport mean free path of probe light propagation in foams and the structure properties of polymer foams are discussed. A probable influence on the optical inversion effect under the wet-to-dry transition in the expanding polymer foams on the diagnostic parameters is taken into account.

## Diffuse reflectance and transmittance measurements

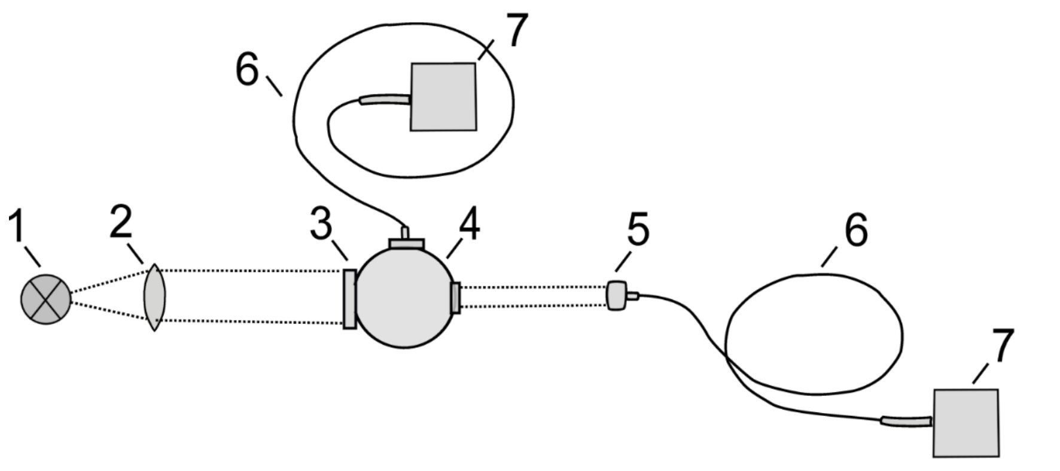

Fig 1. Experimental setup for diffuse and collimated transmittance measurements at long aging times in the spectral range from 500 nm to 900 nm.

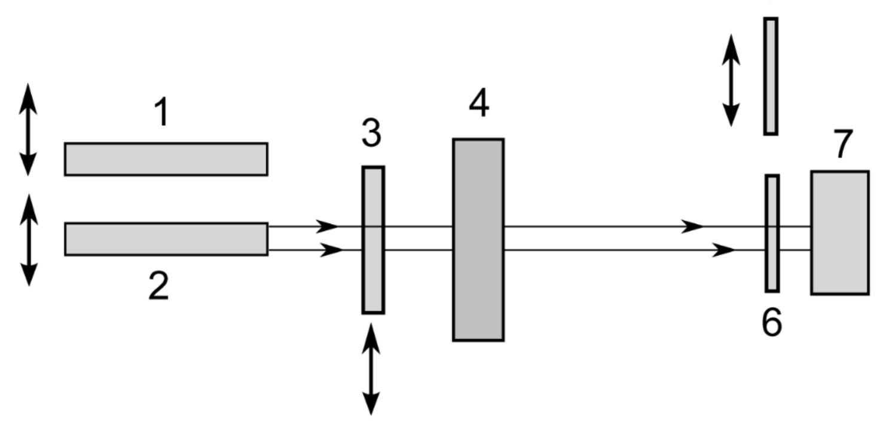

Fig. 2. Experimental setup for collimated (Tc ) transmittance measurements at the fixed wavelengths in the case of small aging times.

$$l(\lambda) = -\frac{L}{\ln\{T_c(\lambda)\}},$$ (Ishimaru A. 1978)

$$l^*(\lambda) = \frac{T_d(\lambda)L}{(1+z_0) - 2T_d(\lambda)z_0},$$ (Sebbah P. 2001)

$$\boldsymbol{g = \frac{l^* - l}{l}}$$

### The model for interpreting the behavior of the scattering anisotropy parameter observed in experiments

$$g = 1 - \frac{\int_0^{2k_0} F(q)S(q)q^3\,dq}{2k_0^2 \int_0^{2k_0} F(q)S(q)q\,dq}$$

Percus-Yevick model (Wertheim M.S., 1963):

$$\begin{cases} S(qd) = \{1 - nG(qd)\}^{-1}; \\ G(qd) = -4\pi d^3 \int_0^1 s^2 \frac{\sin(sqd)}{sqd}(\alpha + \beta s + \gamma s^3)\,ds, \end{cases}$$

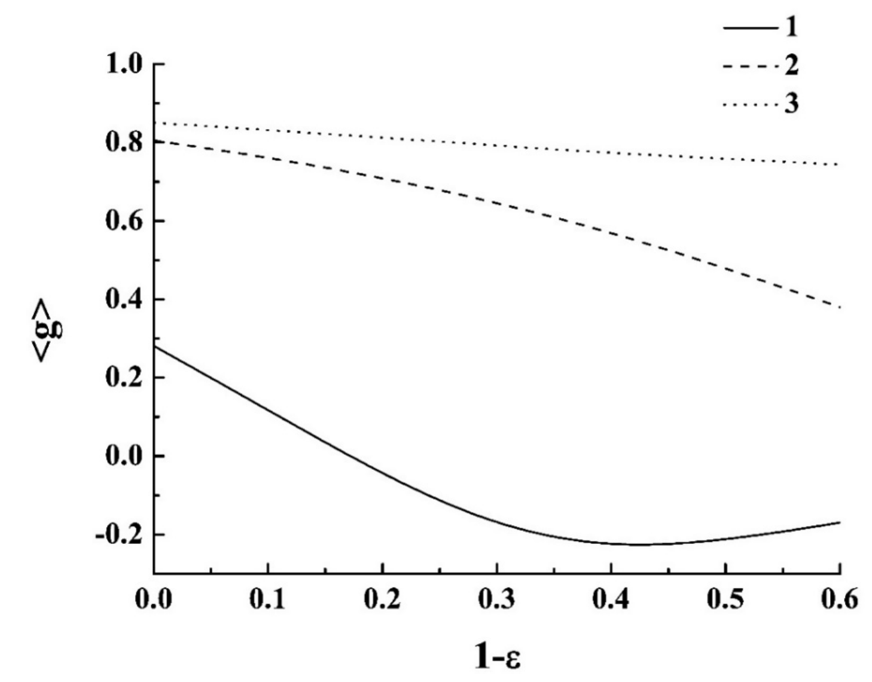

Fig. 3. Percus-Yevick approximation. The wavelength of probe radiation is 633 nm. The refractive index of gas bubbles is equal to 1, the refractive index of the liquid phase is equal to 1.34. Diameters of gas bubbles: 1 - 0.2 µm; 2 - 0.5 µm; 1 - 10.0 µm. The increase in the volume fraction leads to the expected decrease in value of g.

## Low-coherence reflectometry

### Experimental technique

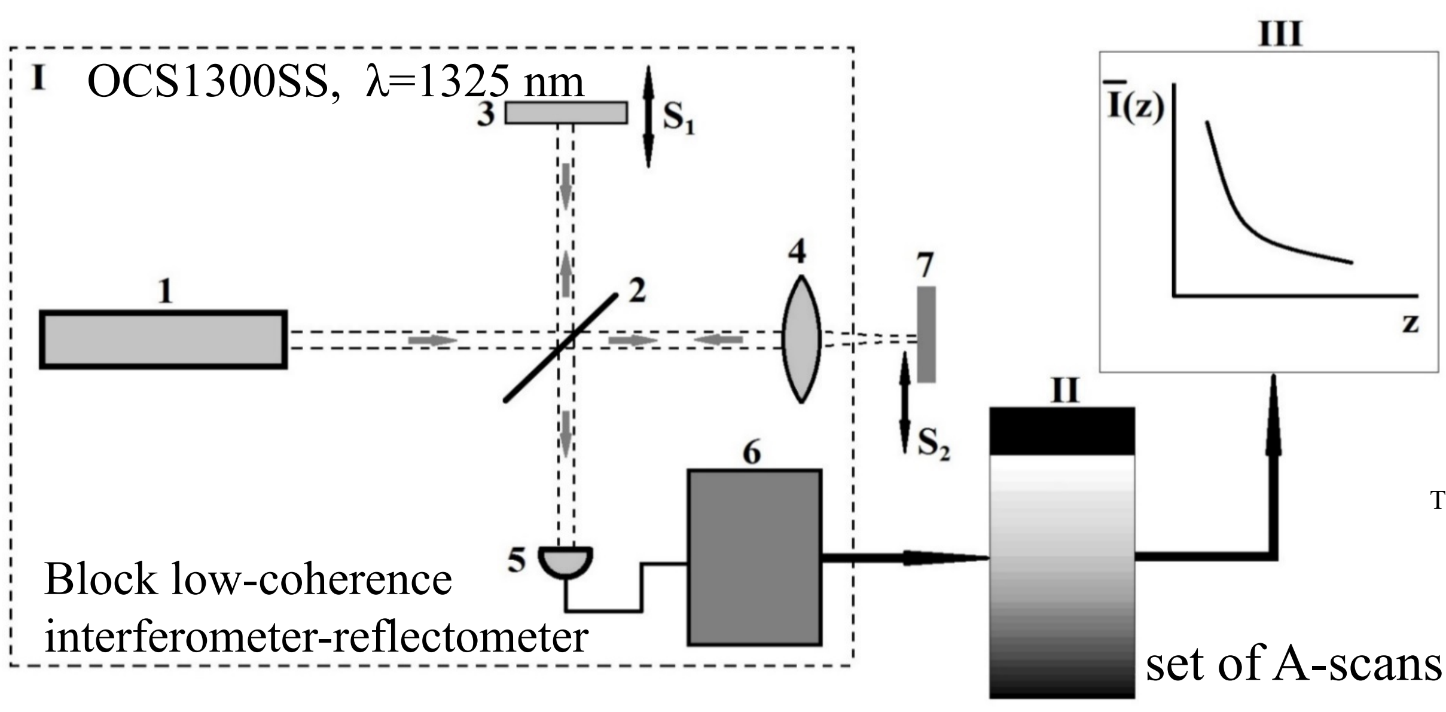

The average intensity of the selected pixel was defined as

Fig. 4. Scheme of low coherence reflectometric sounding of synthesized polylactide matrices (1 - source of low coherent radiation; 2 - a beam splitter; 3 - a mirror in the supporting arm of the interferometer; the optical length of the support arm is modulated according to a periodic law (scan S1); 4 - lens; 5 - photodetector; 6 - block processing the interference signal; 7 - a probed sample used as a diffuse reflector in the object arm of the interferometer; arrow S2 indicates scanning of the sample with a probe beam along the selected direction.

### In the case when $t > \tilde{L}^2/\pi^2 D$

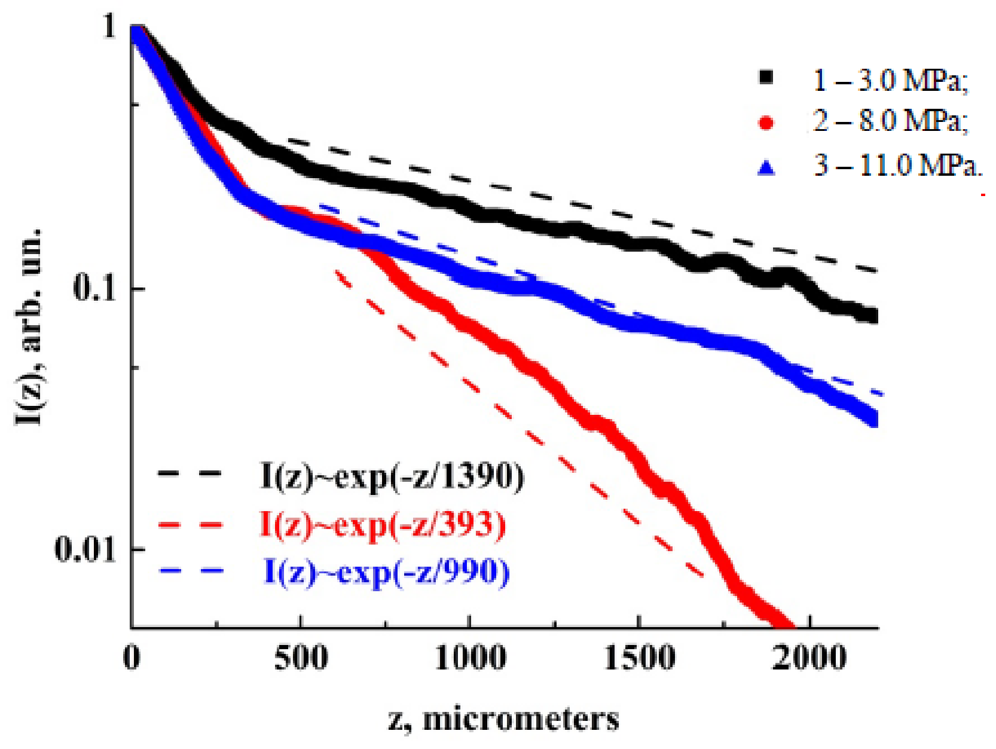

Fig. 5 Typical dependencies of the normalized reflectometric signal on the scan depth for synthesized polylactide matrices. The initial temperature is 309.16 K in all cases.

$$I_d(z) \sim \exp(-z/\xi),$$

where $\xi \approx (3/\pi^2)\cdot(n_{eff}\tilde{L}^2/l^*)$

$$z = v_g t \approx ct/n_{eff}$$

$\boxed{l^*}$ - the transport mean free path of the light propagation

### The methods of Low-coherence reflectometry

The time response of an optically thick layer in the diffusion approximation:

$$I(t) \sim \frac{3D}{l^*\tilde{L}}\cdot\exp\left(-\frac{t}{\tau_a}\right)\cdot\sum_{n=1}^{\infty}\left\{\exp\left(-\frac{D\pi^2 n^2}{\tilde{L}^2}t\right)\cdot\left[1-\cos\left(\frac{l^*+l^*Z_1}{\tilde{L}}\cdot 2\pi n\right)\right]\right\},$$

$t < \tilde{L}^2/\pi^2 D$

$$\boxed{I(t) \sim t^{-3/2}}$$

$t \approx \tilde{L}^2/\pi^2 D$

**Crossover between the two modes of I(t) decay**

$t > \tilde{L}^2/\pi^2 D$

$$\boxed{I(t) \sim \exp(-t/\tau_d),\ \tau_d \approx 3\tilde{L}^2/\pi^2 l^* v_g}$$

### In the case when $t_{max} > \tilde{L}^2/\pi^2 D$

A method for determining the transport length is used the results of Monte Carlo simulation of the similar systems temporal response in the transition between two characteristic modes of the response attenuation and the values of the normalized reflectometric signal obtained in experiments with a probing depth equal to the geometric thickness of the sample.

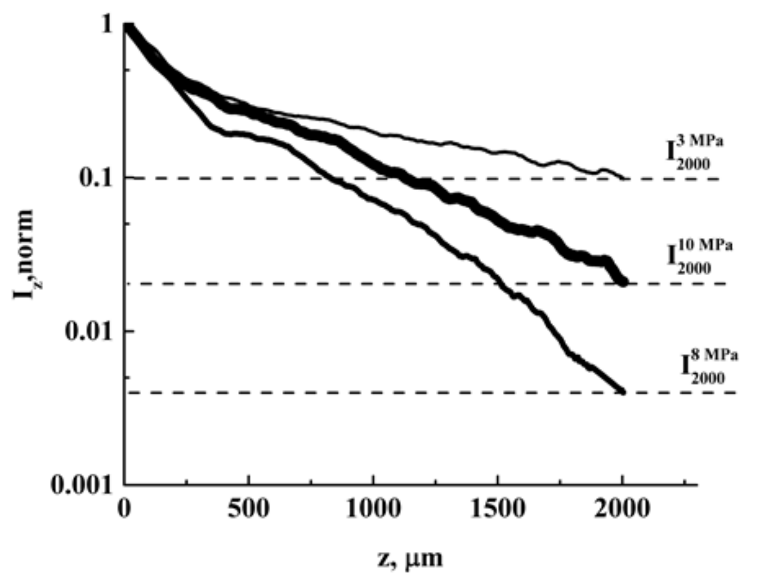

Fig. 6 Typical dependencies of the normalized reflectometric signal on the scan depth for synthesized polylactide matrices. The initial temperature is 309.16 K in all cases.

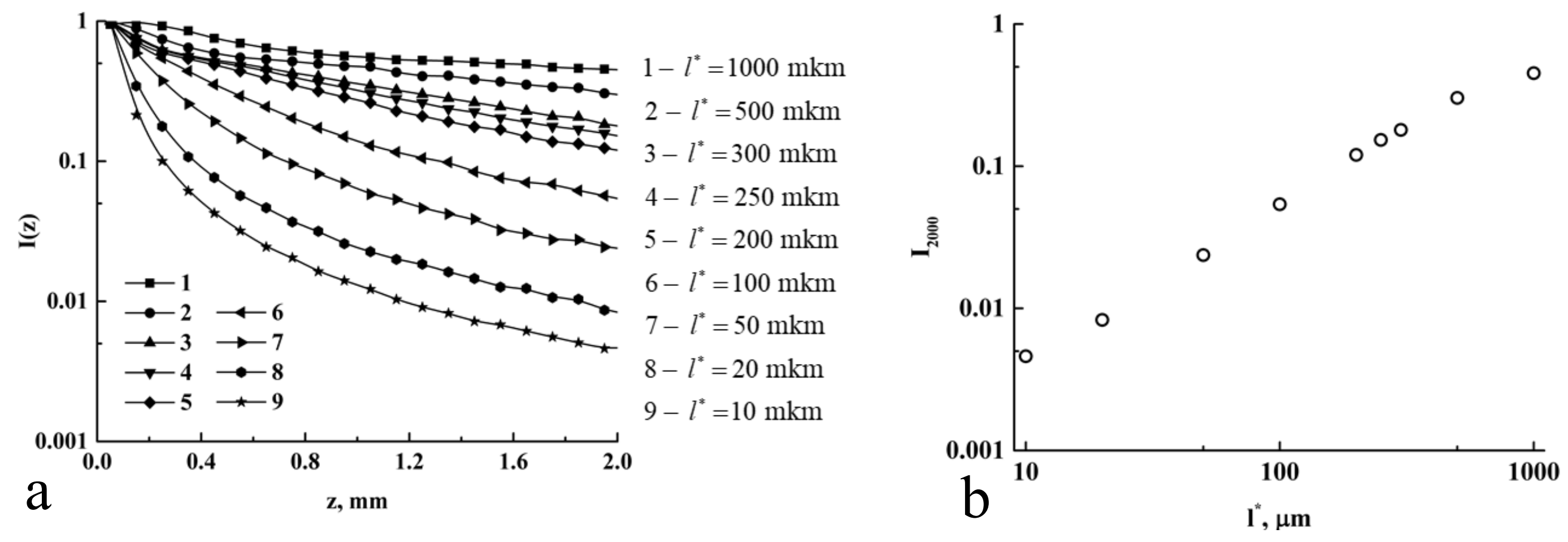

Fig. 7 **a** -Theoretical dependences of the LCR signal intensity on the sounding depth of randomly inhomogeneous layers 2 mm thick with different values of the transport length of radiation propagation in the layer (the results of Monte Carlo simulation ); **b** - Theoretical values of the parameter $I_{2000}$ characterizing the LCR signal attenuation in the probed layers, on the transport length of radiation propagation in the layer. Typical dependencies of the normalized reflectometric signal on the scan depth for synthesized polylactide matrices. The initial temperature is 309.16 K in all cases.

$\boxed{l^*}$ - the transport mean free path of the light propagation

D. Durian et al. (Vera M.U., Saint-Jalmes A., Durian D.J. Applied Optics. 2000.) experimentally obtained the following empirical relationship between the transport length of radiation propagation in the foamed liquid and the average size of gas bubbles (pores) <D> in the foam : $\boxed{\frac{l^*}{\langle D\rangle} \approx \frac{1}{\sqrt{\varepsilon}}}$

## Full-field multi-speckle correlometry

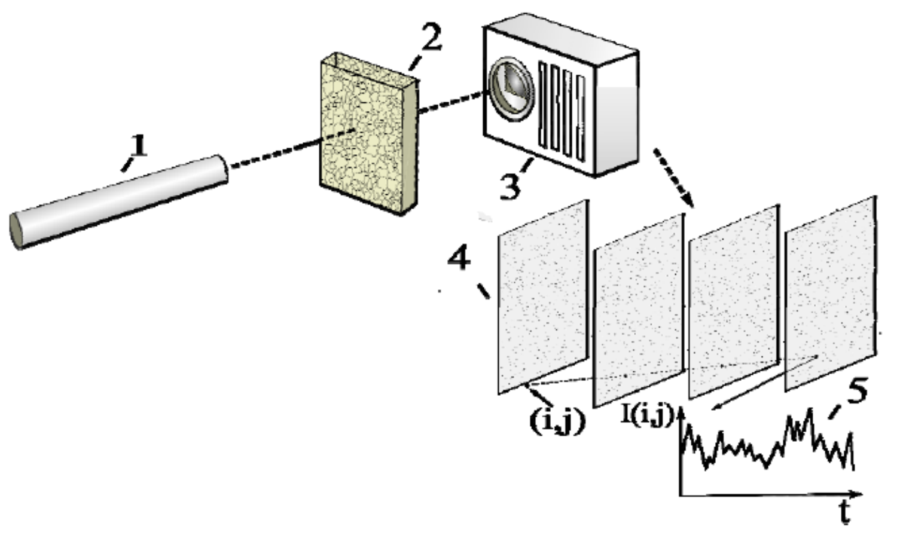

Fig. 8 The scheme of experimental setup: 1 – single-mode He-Ne laser (633 nm, 3 mW, linearly polarized output); 2 – isolated foam sample in the cuvette; 3 – high-performance CMOS sensor; 4 – sequencies of obtained spekle-modulated images; 5 – an example of intensity fluctuations for an arbitrarily chosen pixel in the image plane.

The normalized temporal correlation functions of intensity fluctuations for various image sequences was calculated as:

$$g_2(i,j,\Delta k) = G_2(i,j,\Delta k)/G_2(i,j,0)$$

$$G_2(i,j\cdot\Delta k) = \sum_{k=k_1}^{k_2}\left[I^{k+\Delta k}(i,j) - \bar{I}(i,j)\right]\cdot\left[I^k(i,j) - \bar{I}(i,j)\right]$$

The average intensity of the selected pixel was defined as:

$$\bar{I}(i,j) = \sum_{k=k_1}^{k_2}\frac{I^k(i,j)}{k_2 - k_1}$$

The correlation time of speckle intensity fluctuations c $\tau_C$ was calculated using the obtained values of normalized intensity correlation function $g_2(i,j,\Delta k)$.

The dependence of correlation time of speckle intensity fluctuations was compared with the behavior of the “dispersion parameter” D of the bubble ensemble. The “dispersion parameter” D was calculated as follows:

$$D = \frac{\sigma_r}{\langle r\rangle}$$

where $\sigma_r$ is the standard deviation of the bubble radius, and $\langle r\rangle$ is the average radius.

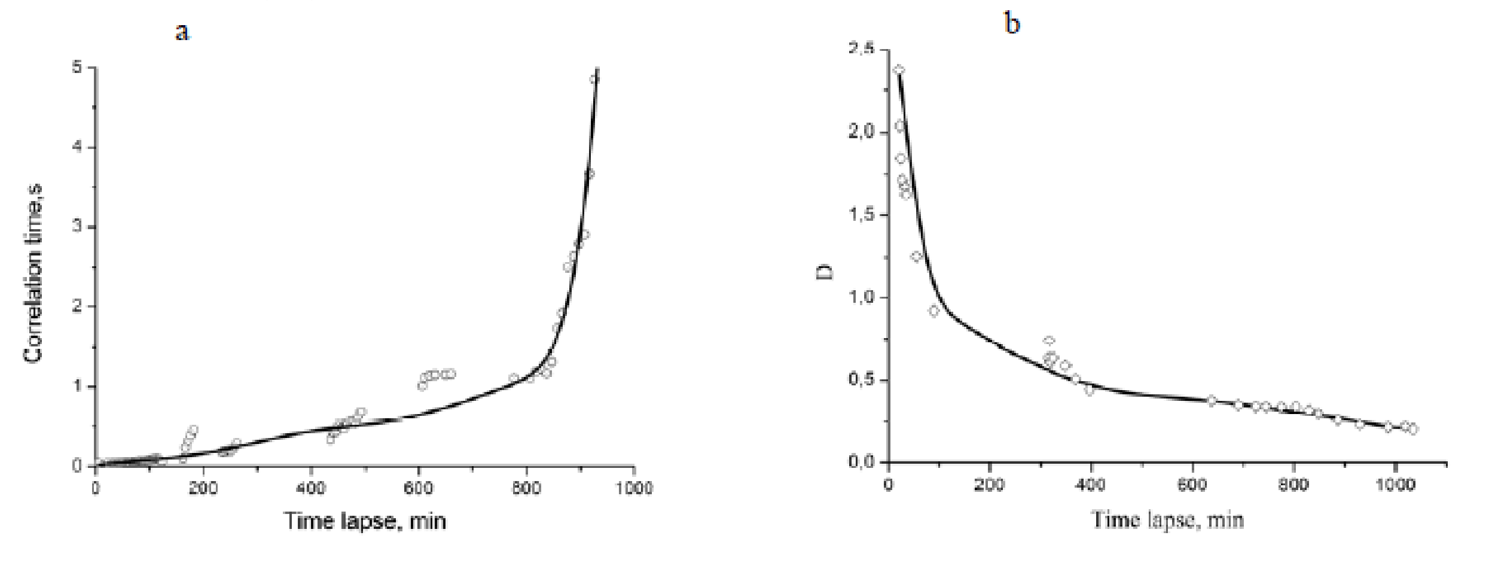

Fig. 9 a) The dependence of standard deviation of the correlation time on the time lapse in the course of foam aging; b) the dependence of normalized standard deviation of the bubble radius on the time lapse in the course of foam aging (E.A. Isaeva, et. al, 2018).

## Conclusion

Various approaches to optical diffusion characterization of growing polymer foams as a specific version of multiple scattering random media with a high level of disorder are demonstrateed their high diagnostic potential as applied to SCF technologies.

*This work is supported by grant from the Russian Foundation for Basic Research (RFBR) # 18-29-06024 MK*